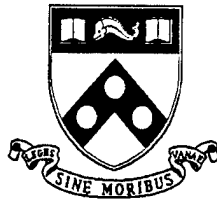


UNIVERSITY of PENNSYLVANIA



ELECTRICAL ENGINEERING DEPARTMENT

11-th Quarterly Report

BIOMORPHIC NETWORKS FOR ATR AND
HIGHER-LEVEL PROCESSING

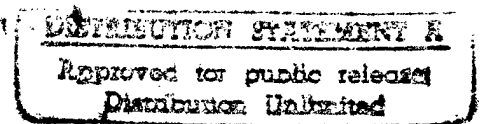
Period covered: 7/01/97 - 10/01/97

Submitted to:
Office of Naval Research
W. Miceli - Scientific Officer

Grant No: N00014-94-0931

Prepared by:

Nabil H. Farhat, Principal Investigator



19971007 175

October 1, 1997

1. BACKGROUND

There is considerable evidence that the basic functional unit for higher-level processing in the cortex is the netlet or *neuronal assembly/(pool or group)* [1]-[10]. This includes extensive analytical and modeling work of netlets carried out independently by several groups. Nearly all this work points to the possibility that netlet dynamics, namely its evolution in time, can be described by the discrete time evolution of the activity $A(n)$, which is the percentage of neurons active at any instant of time. Plots of $A(n+1)$ vs. $A(n)$ obtained under a range of circumstances and assumptions are found to invariably resemble a distorted version of the quadratic or logistic map. The Logistic map is a nonlinear iterative map on the unit interval that exhibits complex orbits depending on the value of nonlinearity (control or bifurcation) parameter of the map [11]. The similarity between the netlet's return map $A(n+1)$ vs. $A(n)$ and that of the logistic map has also been noted by Harth [10] who also mentions that complex and unpredictable sequences $A(n)$ were observed in some of their early simulations of netlets suggesting that certain regions of the netlet's parameter space may have led to observation of chaos in addition to the periodic and fixed point modalities they usually observed.

In light of this evidence we have conjectured that cortical networks can be modeled and numerically studied in an efficient way by means of coupled populations of logistic processing elements [12]. To test this conjecture we have studied the dynamics of such a network when it is subjected to external stimulus patterns that change in time. The networks we study differ from Kaneko's coupled map lattices (CMLs), [13]-[14], in several ways: (a) The networks described here employ parametric rather than the diffuse coupling used in CMLs, (b) The coupling is nonlinear representing the possibility that the interaction between netlets can depend on the activity of the netlets and on the number of active fibers connecting one netlet to another, (c) Our parametrically coupled logistic nets (PCLNs) can be externally driven by time varying or stationary patterns, or by composite patterns that are partially time varying and partially stationary, (d) In the PCLN, control over network dynamics is gradually handed over from initially entirely extrinsic control to eventually entirely intrinsic control. This handing over of control over network dynamics from extrinsic to intrinsic is biologically plausible and is inspired by the remarkable biophysical observation made by Freeman and coworkers [15] regarding gradual disappearance of the trace of a sensory stimulus applied to the olfactory bulb of rabbit as it was followed deeper in the sensory cortex where it was found to eventually vanish in a sea of intrinsically dominated activity. Similar behavior has apparently been observed by Freeman's group in other sensory modalities.

2. PRESENT RESEARCH

The preceding remarks suggest that networks of parametrically coupled logistic maps are biomorphic in the sense that they offer an efficient way to study the functional complexity of cortical networks in order to understand the way they perform higher-level functions. Such higher-level functions are beyond the capabilities of present day sigmoidal networks, and incorporating them in artificial network offers a way for increasing their processing power and for widening their scope of application.

One objective of our research program in biomorphic neural networks and their applications has been to develop networks that: (a) possess biomorphic processing elements whose operation mimics that of the basic functional unit in the brain (cortex), (b) are naturally suited for receiving and processing spatio-temporal inputs (time varying patterns) and can be trained to classify, recognize, or generate such patterns, (c) are able to

compute with diverse state-space attractors that include static (fixed-point) and dynamic attractors with the latter including period-m, and chaotic attractors. This last requirement is motivated by the observation that the brain is essentially a high-dimensional nonlinear dynamical system that can exhibit, in principles all three types of attractors, fixed-point, periodic and chaotic, in its operation, (d) ability to undergo bifurcation (sudden switching) between state-space attractors. Such bifurcation can be a source for versatility and possible source for innovation through chaotic search for novel solutions in the state-space of the PCLNs.

Most sensory information we deal with in daily life is seldom static but is usually dynamic producing patterns of sensory activity that are perpetually changing in time. This occurs in all sensory modalities: seeing, hearing, olfaction (smell), and touch. Similarly most signals produced by the brain to control motor function are spatio-temporal in nature. A similar situation is expected to apply in advanced artificial neural networks intended for higher-level processing. Such network are expected to find application in the processing of spatio-temporal signals of the kind encountered for example in radar, sonar, and speech. They are also expected to be able to generate input specific spatio-temporal signals in response to specific static or dynamic input (stimulus) patterns which is desirable for robotic systems especially when hardware compactness and power efficiency are required. This will be analogous to central pattern generation in the nervous system needed to control movement in living things.

Particularly interesting to us are networks that can accept spatio-temporal signals like those produced in remote sensing and recognition tasks as in radar and sonar. Success in this arena can be useful in other areas and can lead to systems that could recognize continuous speech, or could directly convert spoken commands into complex spatio-temporal control functions. For this reason we have been studying the behavior of parametrically coupled networks of bifurcation processing elements or cells. The focus has been on parametrically coupled networks of logistic maps, for the reasons given earlier but other iterative maps on the interval like the sine-circle (standard) map can also be used.

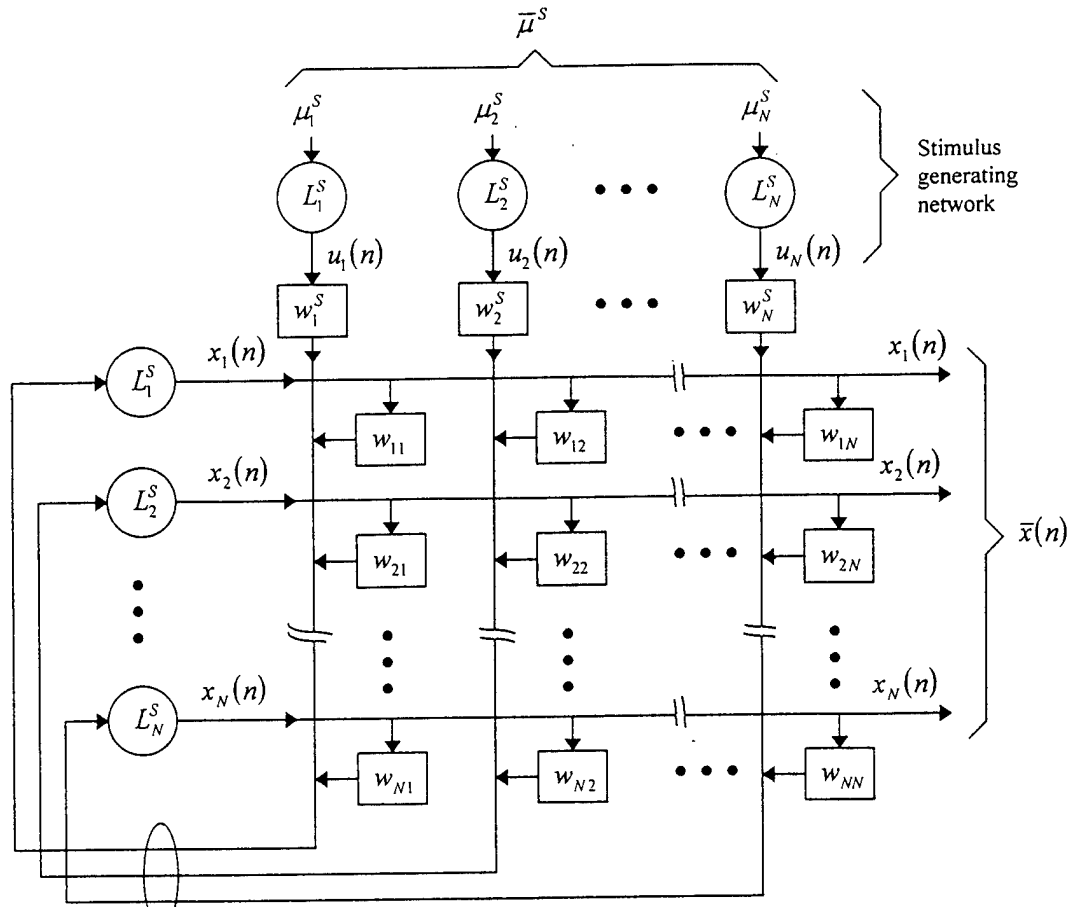
This report is meant to summarize and present a number of recent novel results that have important implications. They were obtained during the past quarter in numerical simulation of PCLNs under external stimulus.

The network studied is shown in Fig. 1. It consists of N parametrically coupled logistic maps arranged on a line (one dimensional geometry) to simplify the display of their time evaluation as will be illustrated below. Parametric coupling means the nonlinearity, (control or bifurcation parameter μ_i of the i-th map is modulated. In the network μ_i is modulated by both extrinsic and intrinsic influences according to

$$\mu_i(n) = \epsilon(n)g_i^s(n) + \frac{1 - \epsilon(n)}{2N_i} \sum_{j=i-N_i}^{i+N_i} g_{ij}(n), \quad \dots i = 1, 2, \dots, N \quad (1)$$

$$\epsilon(n) = \epsilon_0 \exp(-\alpha n)$$

In eq. (1) the first term represents the extrinsic (sensory) input to the i-th logistic processing element or cell and the second term represents the net intrinsic input to the i-th cell through feedback from all other cells connected to it. In eq. (1) n is discrete integer time, $2N_i$ is the number of logistic cells connected to the i-th cell i.e. the number of cells falling within the "connection radius R_c " which is taken to be the same for all cells,



$$\mu_i(n) = \varepsilon(n)w_i^S(u_i) + \frac{1 - \varepsilon(n)}{2N_i} \sum_{j=i-N_i}^{i+N_i} w_{ij}(x_j),$$

$$\varepsilon(n) = \varepsilon_0 \exp(-\alpha n),$$

where ε_0 is in $[0,1]$ and $\alpha \geq 0$ is positive real number.

w_i^S and w_{ij} are nonlinear activity dependent coupling functions with two possible forms each:

$$w_i^S = \begin{cases} g_i^S(u_i) = 4[u_i(n)]^{c_i^S} \\ B_i^S(u_i) = \text{quantized version of } g_i^S(u_i) \text{ } (N_b \text{ levels}) \end{cases}$$

$$w_{ij} = \begin{cases} g_{ij}(x_i) = 4[x_i(n)]^{c_{ij}} \\ B_{ij}(x_i) = \text{quantized version of } g_{ij}(x_i) \text{ } (N_b \text{ levels}) \end{cases}$$

Fig. 1. Parametrically coupled logistic network (PCLN) consisting of N bifurcation (logistic) processing elements or cells. The network employs (a) novel biologically plausible nonlinear (activity) dependent coupling functions between cells each representing a netlet and (b) a biologically plausible gradual transfer of control over network dynamics from initially totally extrinsic (sensory) control to totally intrinsic control. The network can be driven externally by spatio-temporal inputs provided by the stimulus generating network that employs an array of uncoupled logistic maps to conveniently produce a variety of static, time-periodic, chaotic, or composite signals made of any mix of these three-types of signals. The quantized versions of the coupling functions are useful for studying the coarse-grain dynamics of the PCLN.

$g_i(n) = 4(u_i(n))^{w_i}$ is the extrinsic (sensory) input to the i -th cell with variable $u_i(n) \in [0,1]$ being produced in the simulation for convenience by a sensory logistic map according to: $u_i(n+1) = \mu_i^S u_i(n) (1 - u_i(n))$ with $u_i(0) = 0.5$ and μ_i^S being a fixed control parameter of the i -th stimulus generating logistic map. Selecting μ_i^S in $[0,4]$ enables the production of a wide range of stationary, periodic (period- m) or chaotic patterns $u_i(n)$ or any desired combination of such patterns on i depending on the values one selects for μ_i^S . Thus by changing the control vector $\overline{\mu^S}$ of the N stimulus generating logistic cells, a wide range of spatio-temporal driving signals can be applied to the network. The coupling factor w_i ranges between 0 and ∞ . For example $w_i = 0$ produces $g_i^S(n) = 4$ which means the extrinsic contribution tends to make $\mu_i(n)$ high with the result that the i -th processing cell would tend to be chaotic. On the other hand $w_i = \infty$ yields $g_i^S(n) = 0$, because the state variable u_i of the logistic map is in $[0,1]$. This means that small values of w_i introduce disorder while larger values introduces inhibition. Similarly, the quantity $g_{ij}(n)$ in eq. (1) represents the input from the j -th cell to the i -th cell; it has a form similar to $g_i^S(n)$, namely $g_{ij}(n) = 4[X_j(n)]^{C_{ij}}$ with C_{ij} being in $[0,\infty]$ and $X_j(n)$ is the state variable of the j -th logistic processing cell of the network governed by: $X_j(n+1) = \mu_j(n) (1 - X_j(n))$ where $\mu_j(n)$ is given by eq. (1) and $X_j(n)$ is also in $[0,1]$. Note the nonlinear dependence of $g_i^S(n)$ on $u_i(n)$ and $g_{ij}(n)$ on $X_j(n)$ serves two purposes. One, it confines their combined contribution to $\mu_i(n)$ to the allowable range $[0,4]$, and second, changing the values of w_i and C_{ij} provides control over the level of excitation/disorder or inhibition injected into the dynamics of the i -th cell, and hence into the network as a whole, by the i -th sensory cell or by the j -th processing cell respectively. The parameter α in eq. (1) is a positive real constants whose value determines the speed with which control over the dynamic of the network is handed over from initially entirely control extrinsic to eventually and entirely intrinsic control. A value of $\epsilon_0 = 1$ means that initially the dynamics of the network are totally controlled by the extrinsic (sensory) pattern. The passing of control over network dynamic from initially entirely extrinsic to eventually entirely intrinsic is meant to reflect recent intriguing biophysical finding by Freeman and coworkers concerning the fading and eventual disappearance of the traces of a sensory stimulus as it propagates deeper into the sensory cortex [1]. Similarly the nonlinear coupling function $g_{ij}(X_j(n))$ between cells is biologically inspired as nonlinear activity dependent coupling between netlets is more plausible than linear coupling. Indeed simulation results indicate that nonlinear coupling is essential and has several advantages over linear coupling which is expressed by

$$\mu_i(n) = \min \left\{ \epsilon(n) W_i u_i(n) + \frac{1 - \epsilon(n)}{2N_i} \sum_{j=i-N_i}^{i+N_i} W_{ij} X_j(n), 4 \right\} \quad i = 1, 2, \dots, N \quad (2)$$

We find that when the ranges of w_i and w_{ij} are confined to values that do not violate the requirement of the logistic maps namely that they fall in the interval $[0,4]$ (otherwise $\mu_i(n)$

can have values exceeding 4 which is not allowed by definition of the logistic map), the linear coupling does not work in the sense that the network is extinguished: $X_i(n) \rightarrow 0$.

The PCLN represented by eqs. (1) and (2) is clearly an example of an extremely complex system. The general problem in studying complex systems is selecting or finding the regions in the parameter space of the systems for which meaningful and hence potentially useful behavior can be observed. In our case, meaningful behavior could be for instance behavior similar to that seen in the brain with modern imaging techniques primarily with functional magnetic resonance imaging (fMRI) and positron emission tomography (PET) scans. Especially meaningful would be the emergence in our network of corticomorphic behavior only when the selection of network parameters is guided by broad biological principles of cortical operation and organization. Indeed this is the case for the PCLNs we have studied and this makes the results quite exciting with potential to lead to a new generation of powerful neural networks namely dynamical networks that compute with diverse attractors.

Before we go on to describe the PCLN and give examples of its behavior it is worth listing the specific desirable properties we seek in a dynamical network. These include:

- The spatio-temporal response of the network should be stimulus specific i.e. the response of the network should be able to differentiate between different spatio-temporal input patterns; in brief we wish the response to be stimulus specific.
- Rapid convergence to a steady state pattern.
- Independence of the response from the initial state vector $\bar{X}(0)$ of the network i.e., from $X_i(0) \in [0,1]$, $i=1,2,\dots,N$. Note the initial state $u_i(0)$ of the stimulus generating logistic cells is fixed to allow repeatability and coherence of the spatio-temporal input patterns used (in the simulation below $u_i(0)$ is arbitrarily fixed at 0.5).
- Network response should depend on the coupling coefficients matrix C_{ij} $i,j = 1,2,\dots,N$. Recall C_{ij} sets the form of the activity dependent nonlinear coupling function $g_{ij}(X_j) = 4[X_j(n)]^{C_{ij}}$ between the j -th and i -th processing cell of the network offers a mechanism for adaptation and learning in the network.
- Consistency: small changes in the input stimulus, brought about by small changes in the stimulus generating vector $\underline{\mu}^S$, should not change the response, i.e., many similar input patterns produce the same response or negligible changes in the response. When a learning algorithm is developed, consistency might be expanded to include generalization.
- In the absence of extrinsic (input) stimulus (undriven net), the response of the network should depend on the initial state of the network in a manner analogous to that in conventional recurrent networks (Hopfield-type network) that compute with static (point) attractors. The behavior here would be similar but with dynamic in addition to static attractors occurring. The dependence on initial conditions should exhibit basins of attraction just like conventional point attractor network.

- The network should enable testing scenarios for adaptation and learning, especially those that are holography-like in nature because these may offer rapid “one-shot” learning.
- The behavior should resemble known attributes of cortical nets that is being uncovered by functional imaging methods like PET and fMRI.

As will be demonstrated below, we find that there is indeed a range of biologically plausible network attributes and parameters for which the network in Fig. 1 exhibits the above desirable properties. One such attribute is the use of local instead of the global connectivity used in our earlier work. In the present network a cell (netlets) is connected to its near neighbors that fall within a connection radius of $R_C \in [a, b]$ such that the number of cells N_i within R_C is considerably lower than the size N of the network. Although pools of processing cells (netlets) in the cortex do receive and send long range fibers to communicate with other distant pools, the processing by netlet pools is dominated by local interactions. In earlier simulations that employed global connectivity the network was found to exhibit clustering into a number of phase-locked groups with the cells within a cluster being synchronized. In a network of $N \gg N_i$ cells, we find now that by setting $a = 0, b = 1$ or 2 and selecting the value of $R_C \in [0, b]$ for any cell randomly, the network can be made to exhibit isolated clustering i.e., small size clusters of active cells separated by regions of silent ones. This, as was mentioned earlier, is reminiscent to the images of brain activity observed in fMRI and PET. Cells within an isolated cluster are found to possess a variety of types of orbits, i.e., fixed point period- m , and intermittent, quasi-periodic and even chaotic that depend on the input stimulus and the range of nonlinear coupling function $g_{ij}(X_j)$ used. This is considerably richer behavior than the identical period- m synchronized orbits within a cluster observed in earlier work. Fix-point, period- m and chaotic orbits can coexist within isolated clusters and which type of these orbits is more prevalent can be controlled by selecting the range of the coefficient C_{ij} of the nonlinear coupling functions $g_{ij}(x_j(n)) = 4 (X_j(n))^{C_{ij}}$. The simulation results presented below were obtained for random coupling functions formed by selecting C_{ij} randomly with equal probability in the range $[A, B]$ i.e., $C_{ij} \in [A, B]$. Decreasing A towards zero makes the increases the level of excitation and leads to a tendency of the network to exhibit chaotic orbits within some of the isolated clusters. Increasing the value of B , on the other hand, to values above 1 tend to introduce inhibition in the network by making the cell orbits within the isolated clusters more ordered i.e., of the period- m or fixed-point variety and decreases at the same time the size and number of active clusters and further increase in B can cause all activity in the network to be suppressed. The parameters A and B can thus be used to control the level of excitation and disorder in the network (through A) or the level of inhibition (through B).

At the present, the time resolution of fMRI and PET is not sufficient to resolve temporal activity within the active clusters. It would naturally be very meaningful if future imaging technology would be able to resolve the spatio-temporal and not only the spatial brain activity observed under sensory stimulus.

It is worth noting that clustering into a small number of small isolated pockets of activity can be desirable and beneficial in the study of adaptation and learning algorithms based on mutual information because the sparsity of the resulting mutual information matrix

and the greatly reduced computational effort needed to generate it from the orbits of the active cells in the network.

The initial state vector $\bar{X}(0)$ of the processing elements was selected randomly, i.e., $X_i(0)$ $i=1,2,\dots,N$ was selected randomly with equal probability in $[0,1]$. This is done to ensure agreement with cortical networks where the processing units can be in any state at the instant the cortical network receives the effect of a sensory stimulus or, an input from other cortical networks. The initial states $u_i(0)$ $i=1,2,\dots,N$ of the cells in the stimulus generating network were fixed arbitrarily as mentioned earlier at 0.5 in order to preserve repeatability of the stimulus patterns generated.

A program in Windows was developed to exercise the network of Fig. 1 under a wide range of conditions and parameters to study its complex behavior. The following parameters were defined.

N — number of processing cells. Also equal to the number of stimulus generating cells.

R_c — connection radius selected in the range a,b i.e., $R_c \in [a,b]$ when $a,b \geq 0$ defines the number of neighboring cells a given cell is connected to.

Self-connection — Selects whether a cell communicates with itself or not. If the processing unit in the cortex is a netlet, then because a netlet is composed of a large number of interacting neurons, [1]-[7], self-connection is there. Indeed we find that the interesting behavior of the PCLN described below occurs when the self-connection feature in the program is selected.

Periodic Boundary Condition — Selects whether a circular or line array of cells geometry is used or not. This attribute was found to have little effect on the behavior of the network described below because of the small connection radius used.

α, ϵ_0 — parameters defining the speed with which control over dynamics is passed from extrinsic to intrinsic control. (see eq. (1)).

C_1^s — In $g_{ij}(X_j(n)) = 4(X_j(n))^{C_{ij}}$, C_{ij} is selected randomly in the range $[A,B]$. For the results in Fig. 2 were obtained with $C_{ij} \in [0-3]$ in order to demonstrate chaotic orbits coexisting with other types of orbits.

$X_i(0)$: Initial state of the processing cells selected randomly in $[0,1]$.

Stimulus : Selects a number of distinct shapes for the stimulus generating vector $\bar{\mu}^s$.

Examples of the behavior of the network are given in Fig. 2 for a network of $N=100$ cells (netlets). The cell index is $i=0,1,\dots,99$ arranged vertically. The left most panel given the control or nonlinearity vector $\bar{\mu}^s$ of the stimulus generating network. The values of μ_i^s

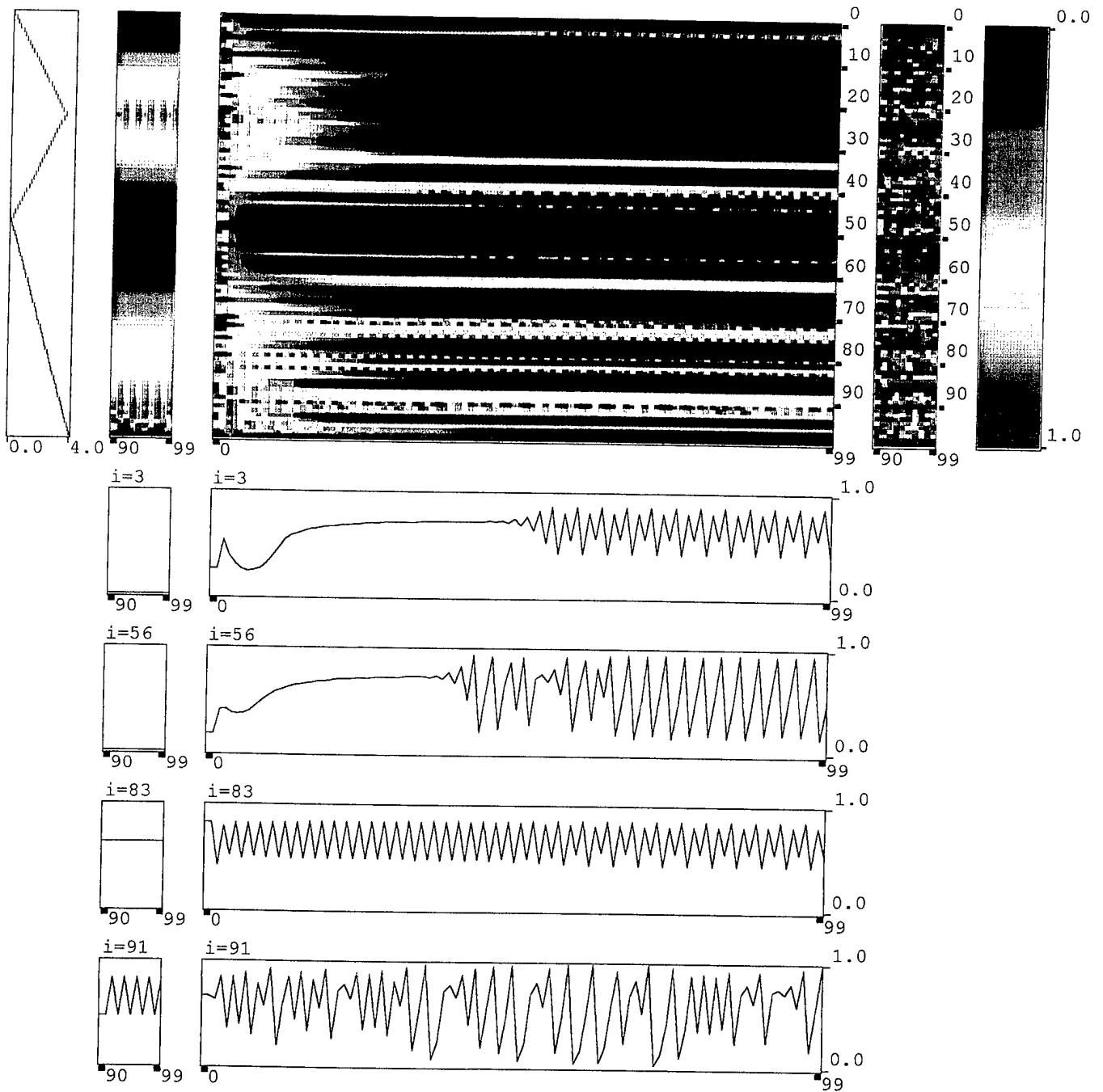


Fig. 2. Example of the behavior of the driven parametrically coupled logistic net of $N=100$ cells. Cells are numbered vertically from $i=0$ to 99 . Each cell has self-connection and is connected to its adjacent cells with probability of $\frac{1}{2}$. The stimulus generating vector $\bar{\mu}^s$ is shown in the left panel, the spatio-temporal pattern $u_i(n)$ produced by the i -th stimulus generating logistic element is shown in the next panel for the $n=90$ to $n=99$ iterations. The central large panel shows the temporal evolution $\bar{X}(n) = \{X_i(n), i = 0, 1, \dots, N = 99\}$ for the first

Figure 2 caption (cont'd)

hundred iterations ($n = 0,1,2,\dots,99$). The initial states $X_i(0)$ for iterating the logistic processing cells was selected randomly in $[0,1]$ and the control parameter $\mu_i(n)$ was that of eq. (1) of the text. Note the rapid emergence of clusters and convergence into "steady state" i.e., persistent types of orbits: for example period-4 orbit for $i=3$, and $i=83$, and chaotic orbit for $i=56$ and 91 . Cells with fixed point orbits encoded by uniform color are easily identified in the central panel. The pattern of isolated clusters shown is specific to the stimulus vector $\bar{\mu}^S$. It is independent of the initial state vector $\bar{X}(0)$ but depends as expected and desired on the matrix of coupling coefficients C_{ij} which was selected randomly in $[0,3]$ in order to allow the appearance of some chaotic orbits within the isolated clusters. (Changing the range of C_{ij} to $[0.3-3]$ eliminates the chaotic orbits and results in isolated clusters containing cells with period- m and/or fixed-point orbits). Other parameters of the network were $\alpha = 0.1$ and $\epsilon_0 = 1$. The convergent pattern of isolated clusters shown in this figure is extended to iteration $n=100-199$ as in Fig. 2(a) which shows that the orbit of $i=56$ is actually intermittent switching between periodic and chaotic episodes.

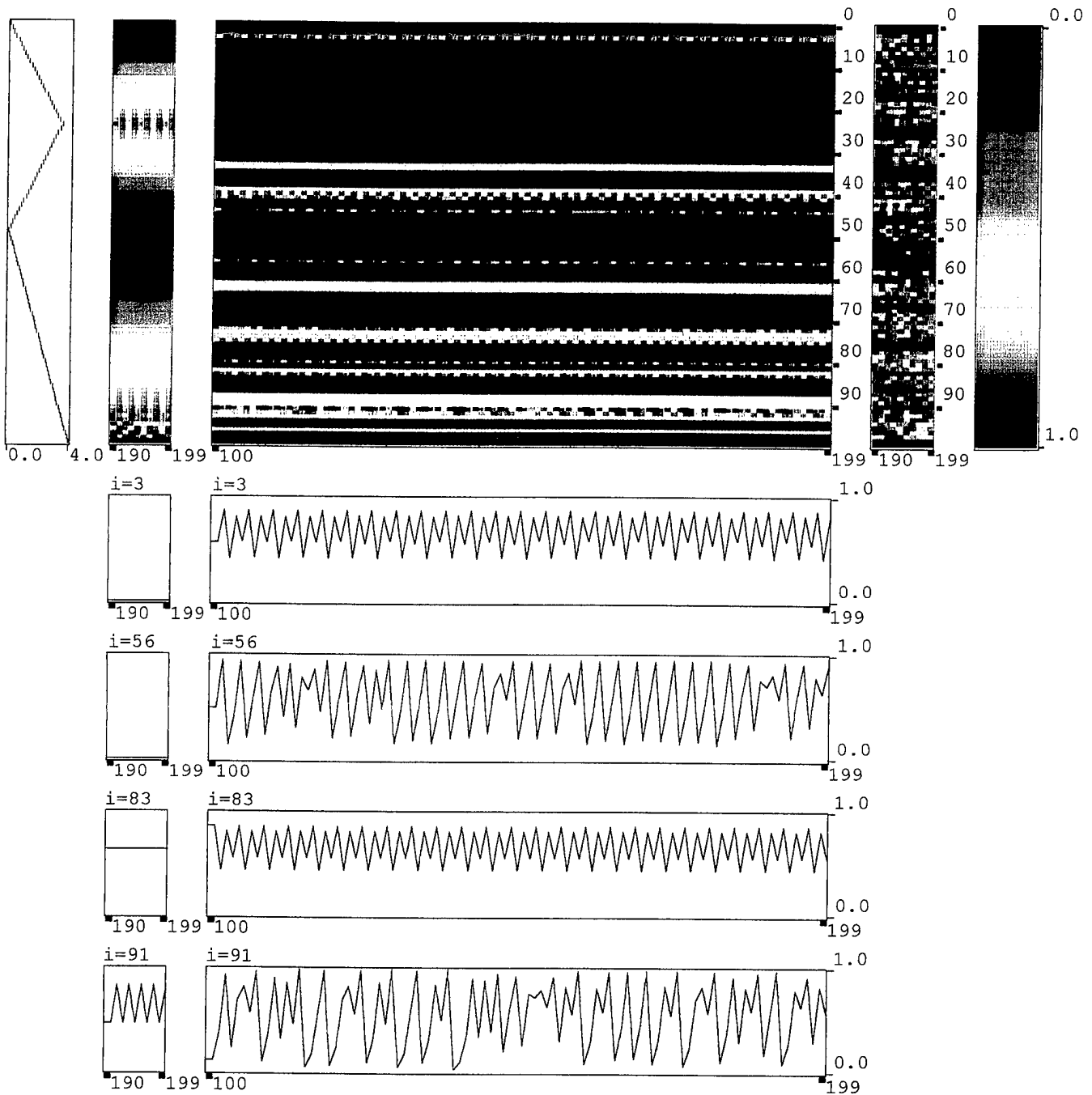


Fig. 2(a). Same as Fig. 2 but for iterations 100-199 to show persistence of the convergent state which continues indefinitely after they appear to about the 60-th iteration (see Fig. 2).

range between [0,4]. The next panel to the right of the $\bar{\mu}^S$ panel is the spatio-temporal input vector $\bar{u}(n)$ with the values of $u_i(n) \in [0,1]$ being color coded in accordance to the color scheme in the extreme right panel. The central large panel gives the time evolution or orbits $X_i(n)$ vs. n , $i=0,1,\dots,N=100$ of the 100 cells of the network i.e., the color coded temporal evolution of the state vector $\bar{X}(n)$ of the network. The first panel to the right of the central panel gives the power spectrum of the state variable $X_i(n)$ treated as a phase-variable, i.e. the power spectrum of $f(X_i) = \exp(j2\pi X_i(n))$ obtained from the Fourier transform of $f(X_i)$ with respect to i formed for every time step n . This is shown for the last 10 iterations of the central orbits plot $X_i(n)$ window i.e., for iterations 90 to 99. The normalized power spectrum is also color coded. We find the power spectrum to be useful in two ways: (a) Conceptually, as projection of the network activity onto a different space, a sort of perception space, (b) observing this window indicates if and when the network converges to a steady periodic state. The presence of disordered or chaotic orbits will produce visible percolation in the power spectrum window. Finally the four panels below the central window give the orbits $X_i(n)$ vs. n for selected cells obtained by specifying any 4 cell numbers i . In this fashion the orbit of an individual cell within any cluster can be examined quantitatively. This also enables us to determine the nature of an orbit i.e., whether it is fixed-point, period- m , or chaotic etc.... Note the qualitative nature of the orbits can also be seen in the central color coded orbits panel. These lower plots illustrate also clearly the initial transient period of the network when $n=0$ to 99 is selected. The range of n covering the 100-199, 200-299 iterations and so on can also be displayed by the program in order to examine the longer term orbits of the network if desired. Normally we find the network converges to a persistent pattern within the first 100 iterations or so, and quite often in 50 iterations.

Most remarkable in the behavior illustrated in Fig. 2 is that the network is capable of classifying spatio-temporal stimulus patterns uniquely and independently of the initial condition of the network at the instant of applying the stimulus. This behavior stems directly from the relinquishing of control over dynamics from initially extrinsic control to eventually entirely intrinsic control. The extrinsic stimulus serves to guide the trajectory of the network with progressively less influence to a region of its state space where it is released to find a "convergent" state compatible with the stimulus. The behavior is also remarkable in that cell orbits of different type (fixed-point, period- m , intermittent, and chaotic) can coexist within the same cluster. The handing over of control over dynamics from extrinsic to intrinsic, is also responsible for the fact that locations of active clusters are not confined to cells associated with high values of μ_1^S but that their locations can cover cells initially receiving very low level of extrinsic activity in a manner that is characteristic of the stimulus pattern.

Another noteworthy aspect of the behavior of the network we have noticed is that there are instances where cells within well separated clusters possess identical synchronized orbits $X_i(n)$ and not just merely phase-locked orbits. This behavior parallels the synchronized oscillations of local field potentials observed by several workers in the brain of cat and monkey and with Eckhorn's modeling of that behavior in networks of spiking neurons[16]-[21].

The independence of behavior from initial conditions may be practically important because it suggests that the network may be able to receive repeated samples of a time varying stimulus pattern to enhance recognition. An example from ATR could be the

broadband echo from a moving aircraft when the repeated samples are from the time evolution of the frequency response or range profile of the target as it changes aspect.

The conceptual similarity of the isolated clustering behavior in PCLNs and the clustering of brain activity seen in fMRI and PET raises an interesting scientific question. If PCLNs are valid models of cortical nets then the clusters of brain activity seen in fMRI and PET should also exhibit analogous temporal activity. Unfortunately the time resolution of fMRI and PET at present is too coarse to discern any temporal activity within the clusters that light-up because both measure the change in blood flow to active brain regions. An increasing number of studies employing PET and fMRI show that different stimuli or cognitive tasks can "light-up" the same brain spot. This strongly suggests a role for temporal encoding to enable differentiation. It would be interesting to see if future technological advances in functional brain imaging could provide the needed temporal resolution to answer this question.

To our knowledge the remarkable behavior of the PCLN outlined in this report has no parallel in sigmoidal neural network, coupled map lattices or cellular automata. Therefore we believe that the use of PCLNs to model cortical networks and higher-level brain functions provide a unique tool for the development of intelligent systems that can operate in a natural environment where time varying signatures are the norm and not the exception.

3. Publications and Conference Presentations:

1. N. Farhat, E. Del Moral Hernandez and G.H. Lee, "Strategies for Autonomous Adaptation and Learning in Dynamical Networks," in Biological and Artificial Computation: From Neuroscience to Technology. J. Mira, R. Morens-Diaz, and J. Cabestany (Eds.), Springer-Verlag, Berlin 1997, pp. 417-426.
2. N. Farhat, "Biomorphic Dynamical Networks for Cognition and Control," *Journal of Intelligent and Robotic Systems*, Kluwer Publishers, (in print). This paper was also presented at NEURAP'97, March 1997.
3. A. Baek and N. Farhat, "Biomorphic Networks for Invariant Feature Extraction," OSA Annual Meeting, Oct. 1997.
4. N. Farhat, "Neuroholography: A Possible Link Between Holography and Cortical Information Processing," OSA Annual Meeting, Oct. 1997.

4. References

1. E.M. Harth, et. al., *J. Theor. Biol.*, vol. 26, pp. 93-120, (1970).
2. P.A. Annios, et. al., *J. Thor. Biol.*, vol. 26, pp. 121-148, (1970).
3. M. Usher, H.G. Schuster and E. Neibur, *Neural Computation*, vol. 5, pp. 370-386, July, (1993).
4. G.M. Edelman, *Neural Darwinsim: The Theory of Neuronal Group Selection*, Basic Books, Inc., Publishers, New York, (1987).
5. C. van Vreeswijk and H. Sompolinski, *Science*, vol. 274, pp. 1724-1726, Dec. (1976).
6. T. Wennekers and F. Pasemann, *International Journal of Bifurcation and Chaos in Applied Science and Engineering*, vol. 6, pp. 2055-2067, (1996).
7. T. Wennekers, F. Sommer and G. Palm, in *Supercomputing in Brain Research: From Tomography to Neural Networks*, H. Hermann, D. Wolf and E. Pöppel (Eds.), World Scientific, Singapore, (1995).
8. G.L. Shaw and D.J. Silverman, in *Computer Simulation in Brain Science*, R. Cotterill (Ed.), Cambridge Univ. Press, Cambridge, (1988), pp. 189-209.
9. M. Shadlen and W. Newhouse, *Opin. Neurobiology*, vol. 14, pp. 569-579, (1994).
10. E. Harth, *Order and Chaos in IEEE Trans. on Systems Man and Cybernetics*, vol. SMC-13, pp. 48-55, (1983).
11. R.C. Hilborn, *Chaos and Nonlinear Dynamics*, Oxford Univ. Press, New York (1994).

12. N. Farhat and E. del Moral Hernandez, "Recurrent nets with recursive processing elements: Paradigm for dynamical computing," SPIE, vol. 2324, SPIE, Bellingham, Wash. (1996), p. 158-170.
13. K. Kaneko, in *Theory and Applications of Coupled Map Lattices*, K. Kaneko (Ed.), J. Wiley, New York, (1993), pp. 1-49.
14. J. Crutchfield and K. Kaneko, in *Directions in Chaos*, vol. 1, World Scientific Publishing Co., Singapore, (1987), pp. 272-353.
15. W.J. Freeman, *Societies of Brains*, LEA Associates Publishers, Hillsdale, N.J., (1995).
16. C.M. Gray and W. Singer, "Stimulus specific neuronal oscillations in the cat visual cortex: a cortical functional unit," Soc. Neurosc., abstr., 404, (1987).
17. _____, "Stimulus dependent neuronal oscillations in the cat visual cortex area 17," Neuroscience, vol. 22, pp. -----, (1987).
18. C.M. Gray, P. Konig, A.K. Engel and W. Singer, "Oscillatory responses in cat visual cortex exhibit inter-columnar synchronization which reflect global stimulus properties," Nature, vol. 338, pp. 334-337, (1989).
19. C.M. Gray and W. Singer, "Stimulus specific neuronal oscillation in orientation columns in cat visual cortex," Proc. Natl. Acad. Sci., USA, vol. 86, pp. 1698-1702, (1989).
20. R. Eckhorn, M. Arndt and P. Dike, "Feature linking via synchronization among distributed assemblies: simulations results from cat visual cortex," Neural Computation, vol. 2, pp. 393-307, (1990).
21. R. Eckhorn and H.J. Reitboeck, "Stimulus-specific synchronization in the cat visual cortex and its possible role in visual pattern recognition," in *Synergetics of Cognition*, H. Haken and M. Stadler (Eds.), pp. 99-111, Springer-Verlag, Berlin, (1990).

| REPORT DOCUMENTATION PAGE | | | Form Approved OMB No. 0704-0188 | |
|---|--|---|------------------------------------|--|
| <small>Public reporting burden for this collection of information is estimated to average 1 hour per response, including the time for reviewing instructions, searching existing data sources, gathering and reviewing the data needed, and completing and reviewing the collection of information. Send comments regarding this burden estimate or any other aspect of this collection of information, including suggestions for reducing the burden, to Washington Headquarters Service, Directorate for Information Operations and Reports, 1215 Jefferson Davis Highway, Suite 1204, Arlington, VA 22202-4302, and to the Office of Management and Budget, Paperwork Reduction Project (0704-0188), Washington, DC 20503.</small> | | | | |
| 1. AGENCY USE ONLY (Leave blank) | 2. REPORT DATE October, 1997 | 3. REPORT TYPE AND DATES COVERED 7/01/97 - 10/01/97 | Quarterly | |
| 4. TITLE AND SUBTITLE BIOMORPHIC NETWORKS FOR ATR AND HIGHER-LEVEL PROCESSING | | 5. FUNDING NUMBERS N00014-94-1-0931 | | |
| 6. AUTHOR(S) Nabil H. Farhat | | | | |
| 7. PERFORMING ORGANIZATION NAME(S) AND ADDRESS(ES) University of Pennsylvania Electrical Engineering Department 200 South 33rd Street Philadelphia, PA 19104-6390 | | 8. PERFORMING ORGANIZATION REPORT NUMBER #11 | | |
| 9. SPONSORING / MONITORING AGENCY NAME(S) AND ADDRESS(ES) Scientific Officer Code: 4414, William Miceli Office of Naval Research, Ballston Tower One 800 North Quincy Street Arlington, Virginia 22217-5660 | | 10. SPONSORING / MONITORING AGENCY REPORT NUMBER | | |
| 11. SUPPLEMENTARY NOTES | | | | |
| 12a. DISTRIBUTION AVAILABILITY STATEMENT | | 12b. DISTRIBUTION CODE | | |
| 13. ABSTRACT (Maximum 200 words) | | | | |
| 14. SUBJECT TERMS | | 15. NUMBER OF PAGES 14 | | |
| | | 16. PRICE CODE | | |
| 17. SECURITY CLASSIFICATION OF REPORT UNCLASSIFIED | 18. SECURITY CLASSIFICATION OF THIS PAGE UNCLASSIFIED | 19. SECURITY CLASSIFICATION OF ABSTRACT UNCLASSIFIED | 20. LIMITATION OF ABSTRACT | |